NANO LETTERS

2005
Vol. 5, No. 9
1638−1642

Effects of Biological Reactions and Modifications on Conductance of Nanofluidic Channels

Rohit Karnik,[†] Kenneth Castelino,[†] Rong Fan,[‡] Peidong Yang,*[,‡,§] and Arun Majumdar*[,†,§]

Department of Mechanical Engineering, University of California, Berkeley, California 94720, Department of Chemistry, University of California, Berkeley, California 94720, and Materials Sciences Division, Lawrence Berkeley National Laboratory, Berkeley, California 94720

Received May 23, 2005; Revised Manuscript Received June 27, 2005

ABSTRACT

Conductance characteristics of nanofluidic channels (nanochannels) fall into two regimes: at low ionic concentrations, conductance is governed by surface charge while at high ionic concentrations it is determined by nanochannel geometry and bulk ionic concentration. We used aminosilane chemistry and streptavidin–biotin binding to study the effects of surface reactions on nanochannel conductance at different ionic concentrations. Immobilization of small molecules such as aminosilane or biotin mainly changes surface charge, affecting conductance only in the low concentration regime. However, streptavidin not only modifies surface charge but also occludes part of the channel, resulting in observable conductance changes in both regimes. Our observations reflect the interplay between the competing effects of charge and size of streptavidin on nanochannel conductance.

Nanofluidic channels and nanopores having dimensions comparable to the size of biological macromolecules such as proteins and DNA have attracted attention in applications such as single molecule detection,[1−4] analysis,[5−9] separation,[10,11] and control[12−14] of biomolecules. Biological nanopores such as α-hemolysin[1] offer single molecule sensitivity but are labile and difficult to handle. On the other hand, inorganic channels are robust and offer better control over channel geometry and are more amenable to integration into functional systems. Nanochannels fabricated in a controlled fashion have enabled the exploration of charge-related effects such as concentration enhancement and depletion[15] and surface-charge-governed transport.[14,16,17] These unique properties of nanochannels arise when the nanochannel size is comparable to either of two length scales: (a) the range of electrostatic interactions in solution and (b) size of the analyte molecules. Since biomolecular analytes are typically charged and have sizes comparable to the above length scales, it is interesting to consider the effects of biomolecular charge and size on transport characteristics of nanochannels under different ionic conditions.

A solid surface in contact with an ionic solution is often charged due the presence of ionized surface groups or adsorbed ions. Counterions accumulate near this charged surface and co-ions are repelled, shielding the surface charge in a characteristic distance known as the Debye length.[18] This length varies with ionic concentration, n, as $l_D \propto n^{-1/2}$, and is typically 1−100 nm for aqueous solutions. Within the Debye layer, the surface charge controls ionic concentrations, which in turn affect the nanochannel conductance that can be calculated for a given surface charge or potential.[16,19] When a 1:1 electrolyte at a bulk concentration of n molecules/m^3 is introduced in a nanochannel of height $2h$ and surface charge σ, the conductance deviates significantly from that of bulk electrolyte when σ/eh is comparable to n (ref 16); that is, when the effective concentration of ions required to neutralize the surface charge, σ/eh, is comparable to bulk ion concentration, n, surface charge plays an important role. In the regime of low electrolyte concentration, $\sigma/eh \gg n$, surface charge governs the ionic concentration inside the channel to maintain electroneutrality ($n_\pm = \sigma/eh$), which in turn controls the nanochannel conductance (Figure 1). Thus the nanochannel conductance (G) for a 1:1 electrolyte, neglecting electroosmotic effects is given by

$$G = 2\sigma \frac{\mu_\pm w}{l} \tag{1}$$

Here μ is ionic mobility (subscripts denote cation/anion) and w and l are the channel width and length, respectively. Hence,

* Corresponding authors: Arun Majumdar, e-mail majumdar@me.berkeley.edu; Peidong Yang, e-mail p_yang@berkeley.edu.
[†] Department of Mechanical Engineering, University of California.
[‡] Department of Chemistry, University of California.
[§] Materials Sciences Division, Lawrence Berkeley National Laboratory.

10.1021/nl050966e CCC: $30.25
Published on Web 07/29/2005

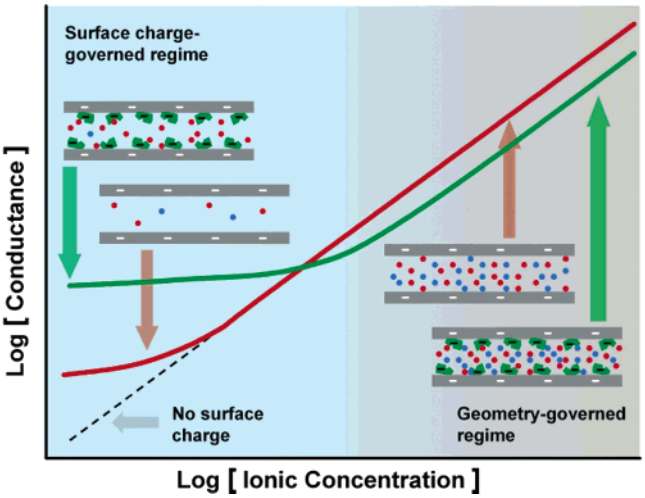

Figure 1. Effect of biomolecules on nanochannel conductance. At high ionic concentrations, nanochannel conductance is governed by channel geometry, while at low ionic concentrations, conductance is governed by surface charge (red curve). Immobilization of biomolecules results in a decrease in conductance at high ionic concentrations due to biomolecule size and an increase in conductance at low concentrations due to biomolecule charge (green curve).

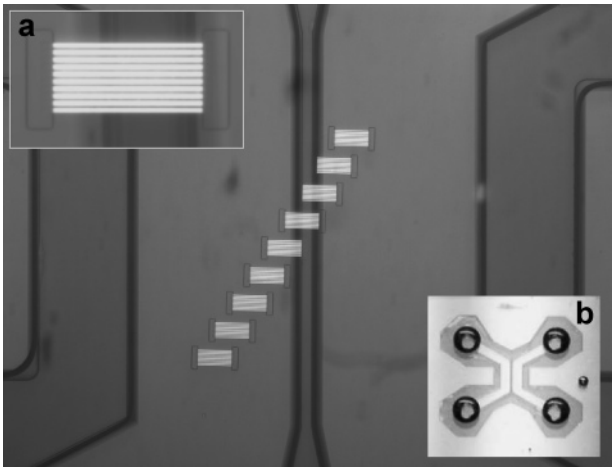

Figure 2. Nanochannel device. Microchannels interface with a single nanochannel device out of a set of staggered devices and enable conductance measurements while providing for good control over electrolyte concentration. Each device consists of 10 120 μm long, 3.5 μm wide, and 30 nm thick silica nanochannels. (Inset a, before etching polysilicon. Inset b, bonded device, showing two microchannels and inlet−outlet ports.)

any functionalization of nanochannel surfaces with different surface groups and biomolecules can be expected to change surface charge and the nanochannel conductance. A signature of this regime is that conductance becomes independent of bulk ionic concentration as well as the channel height. In the high concentration regime, $\sigma/eh \ll n$ and conductance becomes largely independent of surface charge.[14,16] In this regime, conductance depends on channel height and increases linearly with ionic concentration

$$G = 2neh\frac{(\mu_+ + \mu_-)w}{l} \qquad (2)$$

If the size of the biomolecules in the channel is comparable to the channel size, the resulting change in channel geometry (h) would result in a change in nanochannel conductance. Hence, in both regimes, measurement of electrical conductance of nanochannels offers means of probing biological reactions and modifications on surfaces, as illustrated in Figure 1. Electrokinetic measurements in microslits have been used for the characterization of surfaces and measurement of protein adsorption.[20,21] However, electrokinetic characterization is cumbersome, involving the application of pressure and the measurement of flow rates. In nanochannels, surface effects dominate and we can expect biological modifications and reactions to be detected directly by simply measuring the conductance.

To fabricate the nanochannel devices, a 30 nm thick layer of polysilicon was deposited on a fused silica wafer using low-pressure chemical vapor deposition (LPCVD) process and subsequently patterned, forming sacrificial material that defined the nanochannels. Polysilicon film thickness was measured using a Nanospec 3000 film analysis system (Nanometrics) as well as with an Alpha-Step IQ surface profiler (KLA-Tencor) after patterning the thin film. A 2 μm thick low-temperature oxide was then deposited in a LPCVD process, annealed, patterned, and etched down to access the nanochannel ends. Microchannels with access holes were fabricated on another fused silica wafer. The nanochannel and microchannel components were then bonded together using a transfer bonding technique with poly(dimethylsiloxane) (PDMS) (Sylgard 184, Dow Corning) as adhesive.[22] A number of staggered nanochannels were used in the fabrication process such that only one set of nanochannels bridged the microchannels. After bonding, nanochannels were formed by etching the sacrificial polysilicon with xenon difluoride gas at 3 Torr for 1.5 h (Figure 2). Once the channels were formed, the entire device was treated with oxygen plasma at 300 W for 10 min in a plasma etcher (Technics).

Plasma-treated surfaces of the channels were immersed in a 2% solution of (3-aminopropyl)trimethoxysilane (APTMS) (Gelest Inc.) in ethanol for 1 h at room temperature, followed by a 5-min ethanol rinse. The devices were then immersed in a 0.1× phosphate-buffered saline (PBS, pH 7.2, Invitrogen; 10× PBS is an aqueous solution of 1.55 M NaCl, 0.015 M KH_2PO_4, and 0.027 M Na_2HPO_4). Biotinylation of the surface was done by treating the aminosilane-coated surface with a 10 mM solution of Sulfo-NHS-SS-Biotin (sulfosuccinimidyl 2-(biotinamido)-ethyl-1,3-dithiopropionate) (Pierce Biosciences) in 0.1× PBS for 1 h at room temperature. The succinimide moiety reacts readily with the primary amine group of the APTMS resulting in cross-linking biotin to the surface. The NHS-SS-biotin cross-linker was used because of its long spacer arm, which reduces steric constraints leading to better binding efficiency of avidins. Residual amine groups, if any, were then passivated by treating the surface with a 10 mM solution of *n*-hydroxysuccinimide (NHS) (Sigma Aldrich) in 0.1× PBS for 1 h at room temperature.

Following each step of surface reactions, electrical conductance of the nanochannels was measured at a range of

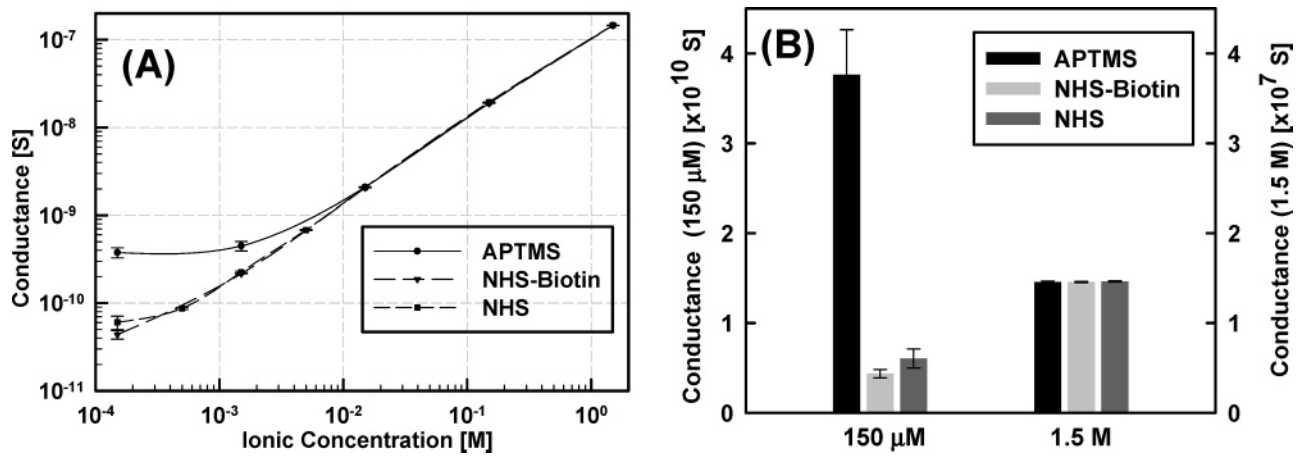

Figure 3. Changes in nanochannel conductance after various steps of surface functionalization. (A) APTMS functionalization resulted in high conductance at low ionic concentrations. This conductance dropped to 11% of its original value upon treatment with NHS−biotin. Subsequent treatment with NHS increased conductance slightly. No appreciable change in conductance was observed at high ionic concentrations indicating absence of steric blocking. (B) Detailed plot of conductance at the highest and lowest buffer concentrations. The error bars (1σ) correspond to five measurements at each point. PBS buffer was used for the measurements ($1\times$ PBS corresponds to an ionic concentration of 0.15 M).

buffer concentrations using a Keithley 6430 sub-femtoamp source meter controlled through a GPIB interface by a real-time control and analysis MATLAB program. Ag/AgCl electrodes were used to make electrical contact with solutions through access holes at the ends of microchannels. While solutions were changed, conductance measurements and rinses were carried out alternately to ensure complete rinsing.

Nanochannel conductance for a range of concentrations from $0.001\times$ to $10\times$ PBS after each step of surface modification is shown in Figure 3A. This device was first treated with APTMS, followed by NHS-SS-biotin and then NHS. At higher buffer concentrations, conductance varied linearly with concentration. Approximating $10\times$ PBS as 1.55 M NaCl with an equivalent conductivity of 10^{-2} m^2 S/mol[23] (or $\mu_+ + \mu_- = 10.4 \times 10^{-8}$ m^2/(V s)) and device geometry of 10 parallel 120 μm $\times$ 3.5 μm $\times$ 30 nm channels (first two dimensions estimated from micrographs), eq 2 gives an expected conductance of 1.35×10^{-7} S, which is in reasonable agreement with the measured nanochannel conductance under the same conditions. The conductance was repeatable from device to device, confirming the integrity of nanochannels and the microchannel interface. However, at low buffer concentrations, nanochannel conductance deviated significantly from linearity and was seen to level off for the APTMS treated nanochannels. At pH 7.2, the amino groups may be expected to be positively charged. Assuming that the conducting ions are Cl^- with a mobility of 7.9×10^{-8} m^2/(V s), the estimated surface charge is approximately 8 mC/m^2. In this case, σ/eh corresponds to about 5 mM, which is much larger than the bulk concentration of $\sim$150 μM and hence $\sigma/eh \gg n$. Treatment with NHS-SS-biotin drastically lowered conductance at low buffer concentrations, presumably due to reaction of the amino group with the NHS group resulting in a moiety with no charge. In this case, surface charge was lowered to such an extent that and σ/eh is comparable to n and eqs 1 and 2 are not valid. However, since conductance decreases monotonically with bulk concentration, eq 1 puts an upper bound of about 1 mC/m^2 on the surface charge. Further treatment with NHS did not result in a large change in conductance. To clearly illustrate charge-governed and geometry-governed regimes, conductance values at $10^{-3}\times$ and $10\times$ PBS ($\sim$150 μM and 1.5 M NaCl) for the three surfaces are shown in Figure 3B. It is seen that functionalization of nanochannel surfaces with small molecules resulted in a large change in surface charge, detected at low buffer concentrations, while conductance values at high buffer concentration remained unchanged, indicating no change in nanochannel geometry.

To study the effect of biological binding reactions on nanochannel surfaces, 1 mg/mL Alexa Fluor 488 labeled streptavidin (Molecular Probes, Eugene, OR) in $0.1\times$ PBS was introduced into the above test device for 10 h at room temperature, followed by rinsing in buffer. To ensure that any observed changes were not due to effects external to nanochannels such as blocking of nanochannel inlets, another nonbiotinylated control device was prepared by treatment with APTMS followed by NHS and was similarly treated with streptavidin. Use of fluorescently labeled streptavidin enabled electrical measurement as well as direct optical confirmation of the presence or absence of streptavidin on nanochannel surfaces. Conductance measurements (Figure 4) revealed large changes in conductance of the biotinylated nanochannels (test device) at both low and high ion concentrations, but little change in conductance of the nonbiotinylated nanochannels (control device). Further, this is corroborated by fluorescence images obtained with a Nikon TE2000-U inverted epifluorescence microscope using an ORCA-ER (Hamamatsu Photonics Gmbh) camera, which clearly showed immobilization of streptavidin in the test device but not in the control device (Figure 4, insets).

Conductance measurements in charge-governed and geometry-governed regimes (Figure 5) reveal that immobilization of streptavidin in the nanochannels resulted in changing not only the surface charge but also the device geometry. At $10\times$ PBS, conductance of the biotinylated nanochannels dropped by about 15% when streptavidin was introduced,

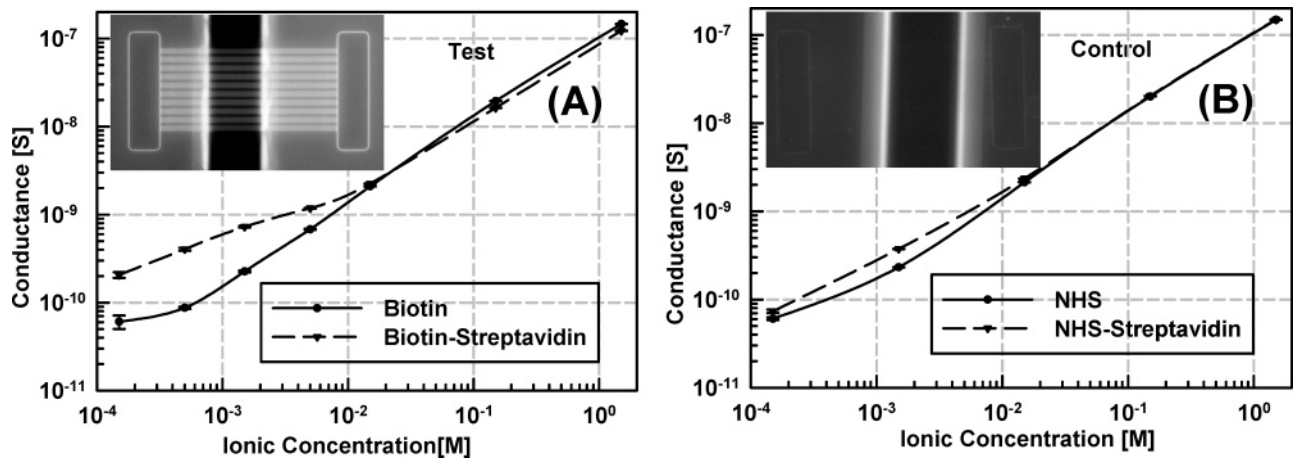

Figure 4. Streptavidin−biotin binding reaction. (A) Conductance response of the test device functionalized with NHS-SS-biotin and passivated with NHS over a range of ionic concentrations. The immobilized fluorescent streptavidin was imaged optically to confirm the binding reaction (inset). (B) Conductance measurements for the control device passivated completely with NHS. No fluorescent signal was observed in this case indicating that streptavidin did not get immobilized on the surface (inset). PBS buffer was used for the measurements (1× PBS corresponds to an ionic concentration of 0.15 M).

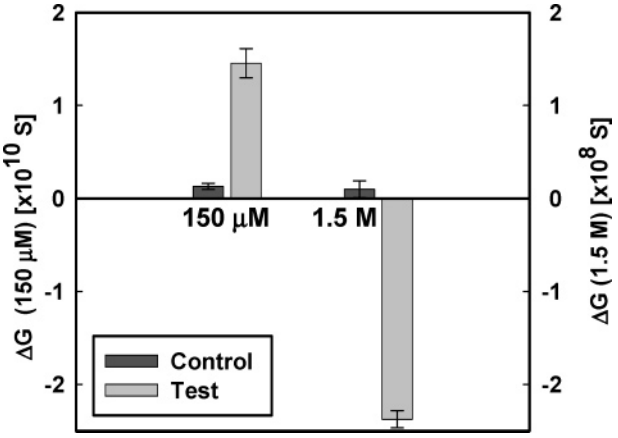

Figure 5. Change in nanochannel conductance in different concentration regimes. (a) At low ionic concentration (150 μM), streptavidin immobilization leads to increased surface charge and hence increased conductance. (b) At high ionic concentrations (1.5 M), streptavidin causes steric blocking of the nanochannels causing a drop in conductance. PBS buffer was used for the measurements (1× PBS corresponds to an ionic concentration of 0.15 M).

indicating an effective reduction in channel size from about 30 to 25 nm or an immobilized layer effectively 2.5 nm thick on the surface. This change is consistent with the globular size of streptavidin (5−6 nm)[24] and the change in size of colloids on protein binding reported in other studies.[25] At low ion concentrations, conductance of the biotinylated nanochannels showed an increase, which implies an increase in the surface charge due to immobilization of streptavidin. Streptavidin with a mildly acidic pI of 5 is reported to have about two electron charges at pH 7.2 (ref 26), which qualitatively explains the increase in conductance. The conductance of the nonbiotinylated nanochannels remained relatively unchanged, indicating that the changes observed in the test device can be attributed to the streptavidin binding reaction.

Our experiments clearly demonstrate that biological binding events modulate surface charge and change nanochannel geometry. Moreover, conductance values were highly repeatable even after rinsing with different buffer concentrations. At the lowest buffer concentration, APTMS-treated surfaces showed the largest variability in conductance. This variability may be due to the presence of bivalent phosphate counterions in PBS, since multivalent ions are known to adsorb and sometimes even reverse charge on highly charged surfaces.[18] In contrast, NHS and NHS-SS-biotin treated surfaces were extremely stable after rinsing with different buffer concentrations; conductance varied by less than 10^{-11} S in some cases. Assuming that change in conductance is roughly equivalent to a change in ionic concentration of $\Delta\sigma/eh$, it corresponds to variations in surface charge of approximately 0.1 mC/m^2 or one electron charge per 400 Å × 400 Å area. This observation suggests that electrochemically stable nanochannel surfaces could be used as highly sensitive probes for measuring changes in surface charge. On the other hand, at high ionic concentrations, we observed a variation of about 1% in nanochannel conductance. This could be due to slight variations in concentration and temperature since the viscosity of water changes by 2% per 1 °C change in temperature in the 20−30 °C range,[23] resulting in changes in ionic mobilities and conductance. Since the room temperature remained at 23 ± 0.5 °C during the course of the experiment, these variations are not expected to materially affect the results. Another aspect of streptavidin immobilized on nanochannel surfaces is the deviation of conductance at low concentrations from that of nanochannels with a constant surface charge. This behavior could arise from a number of effects including charge regulation of streptavidin due to changes in pH, discreteness of charge, adsorption of ions, nonplanar geometry due to streptavidin, etc. Moreover, interpretation of electrokinetic characteristics of adsorbed proteins in terms of a Debye layer at a plane surface was shown to be inadequate.[20,27] Further investigations are required to study and explain this behavior.

Our experiments indicate that biomolecule charge and volume have opposite effects on nanochannel conductance: biomolecule charge increases the number of conducting ions

in the nanochannel whereas volume exclusion of ions decreases the number of conducting ions. This argument is valid when the nanochannel has a comparatively low surface charge to begin with, as in the present case. Consider a biomolecule with charge q and volume V present in a solution with ionic concentration n in the nanochannel. The number of charges on the biomolecule is q/e, where e is the charge of an electron. The number of conducting ions introduced due to biomolecule charge is expected to be of the order of q/e, while the number of excluded ions is of the order of nV. These contributions are analogous to eqs 1 and 2, the first contribution depending only on charge and the second one varying with geometry and ionic concentration. The biomolecule charge effect dominates at lower ionic concentration, but as the ionic concentration increases, the number of ions displaced due to the biomolecule volume increases. This exactly offsets the effect of biomolecule charge at a certain concentration, i.e., when $n \sim q/eV$. At higher concentrations, the volume exclusion effect dominates. For streptavidin, using $V = 5.4 \times 5.8 \times 4.8$ nm^3 (ref 24) and $q/e = 2$ (ref 26), we get $q/eV = 22$ mM, which is in agreement with the data in Figure 4A. Interestingly, we observed an analogous transition in the conductance of DNA translocation through nanotubes[28] though the transition occurred at a much higher ionic concentration.

In conclusion, our experiments demonstrate that the ionic conductance of nanochannels reflects an interplay between the competing effects of biomolecule charge and size. Nanochannel conductance could be used to sense surface charge and the presence of biomolecules immobilized on nanochannel surfaces in both surface-charge-governed and geometry-governed regimes. Our devices provide for an integrated nanofluidic platform with a robust electronic probing scheme that is amenable to scaling and multiplexing. This technique could be developed for charge-sensitive biosensing, having the potential of label-free detection of binding of small molecules and kinase activity, which are hard to detect conventionally.

Acknowledgment. We acknowledge the support of Basic Energy Sciences, Department of Energy; the IMAT program of the National Cancer Institute; and the National Science Foundation. R.K. would like to acknowledge Min Yue and Deyu Li for input on device fabrication. We also thank Richard Cote, Ram Datar, Hirofumi Daiguji, and Andrew Szeri for their collaboration. We acknowledge the UC Berkeley Microfabrication Laboratory for the use of their facilities.

References

(1) Kasianowicz, J. J.; Brandin, E.; Branton, D.; Deamer, D. W. *Proc. Natl. Acad. Sci. U. S. A.* **1996**, *93*, 13770−13773.
(2) Li, J.; Stein, D.; McMullan, C.; Branton, D.; Aziz, M. J.; Golovchenko, J. *Nature* **2001**, *412*, 166−169.
(3) Saleh, O. A.; Sohn, L. L. *Nano Lett.* **2003**, *3*, 37−38.
(4) Chang, H.; Kosari, F.; Andreadakis, G.; Alam, M. A., Vasmatzis, G.; Bashir, R. *Nano. Lett.* **2004**, *4*, 1551−1554.
(5) Deamer, D. W.; Akeson, M. *Trends Biotechnol.* **2000**, *18*, 147−151.
(6) Howorka, S.; Cheley, S.; Bayley, H. *Nat. Biotechnol.* **2001**, *19*, 636−639.
(7) Kobayashi, Y.; Martin C. R. *Anal. Chem.* **1999**, *71*, 3665−3672.
(8) Siwy, Z.; Trofin, L.; Kohli, P.; Baker, L.; Trautmann, C.; Martin, C. R. *J. Am. Chem. Soc.* **2005**, *127*, 5000−5001.
(9) Steinle, E. D.; Mitchell, D. T.; Wirtz, M.; Lee, S. B.; Young, V. Y.; Martin, C. R. *Anal. Chem.* **2002**, *74*, 2416−2422.
(10) Han, J.; Craighead, H. G. *Science* **2000**, *288*, 1026−1029.
(11) Jirage, K. B.; Hulteen, J. C.; Martin C. R. *Science* **1997**, *278*, 655−658.
(12) Kuo, T.-C.; Cannon, D. M. Jr.; Chen, Y.; Tulock, J. J.; Shannon, M. A.; Sweedler, J. V.; Bohn, P. W. *Anal. Chem.* **2003**, *75*, 1861−1867.
(13) Nishizawa, M.; Menon, V. P.; Martin C. R. *Science* **1995**, *268*, 700−702.
(14) Karnik, R.; Fan, R.; Yue, M.; Li, D.; Yang, P.; Majumdar, A. *Nano Lett.* **2005**, *5*, 943−948.
(15) Pu, Q. S.; Yun, J. S.; Temkin, H.; Liu S. R. *Nano Lett.* **2004**, *4*, 1099−1103.
(16) Stein, D.; Kruithof, M.; Dekker C. *Phy. Rev. Lett.* **2004**, *93*, 035901−1−4.
(17) Plecis, A.; Schoch, R. B.; Philippe, R. *Nano Lett.* **2005**, *5*, 1147−1155.
(18) Israelachvili, J. *Intermolecular and surface forces*, 2nd ed.; Academic Press: London, 2003.
(19) Levine, S.; Marriott, J. R.; Robinson K. *J. Chem. Soc., Faraday Trans. 2* **1975**, *71*, 1−11.
(20) Werner, C.; Körber, H.; Zimmermann, R.; Dukhin, S.; Jacobasch, H.-J. *J. Colloid Interface Sci.* **1998**, *208*, 329−346.
(21) Norde, W.; Rouwendal, E. *J. Colloid Interface Sci.* **1990**, *139*, 169−176.
(22) Satyanarayana, S.; Karnik, R.; Majumdar A. *J. Microelectromech. Syst.* **2005**, *14*, 392−399.
(23) Lide, D. R. *Handbook of chemistry and physics*, 73rd ed.; CRC Press: Boca Raton, FL, 1992−93.
(24) Hendrickson, W. A.; Pähler, A.; Smith, J. L.; Satow, Y.; Merritt, E. A.; Phizackerley. *Proc. Natl. Acad. Sci. U. S. A.* **1989**, *86*, 2190−2194.
(25) Sohn, L. L.; Saleh, O. A. *Proc. Natl. Acad. Sci. U. S. A.* **2003**, *100*, 820−824.
(26) Sivasankar, S.; Subramaniam, S.; Leckband, D. *Proc. Natl. Acad. Sci. U. S. A.* **1998**, *95*, 12961−12966.
(27) Matsumura, H.; Verbich, S. V.; Dimitrova, M. N. *Colloids Surf., A* **2001**, *192*, 331−336.
(28) Fan, R.; Karnik, R.; Yue, M.; Li, D.; Yang, P.; Majumdar, A. *Nano Lett.* **2005**, *5*, 1633−1637.

NL050966E